

Magnetic field effects and magnetic anisotropy in lightly doped $\text{La}_{2-x}\text{Sr}_x\text{CuO}_4$

M. Matsuda

Advanced Science Research Center, Japan Atomic Energy Research Institute, Tokai, Ibaraki 319-1195, Japan

M. Fujita and K. Yamada

Institute for Chemical Research, Kyoto University, Gokasho, Uji 610-0011, Japan

R. J. Birgeneau

Department of Physics, University of Toronto, Toronto, Ontario, Canada M5S 1A1

Y. Endoh

Institute for Materials Research, Tohoku University, Katahira, Sendai 980-8577, Japan

G. Shirane

Department of Physics, Brookhaven National Laboratory, Upton, New York 11973

(November 14, 2018)

The effects of the application of a magnetic field on the diagonal stripe spin-glass phase is studied in lightly doped $\text{La}_{2-x}\text{Sr}_x\text{CuO}_4$ ($x=0.014$ and 0.024). With increasing magnetic field, the magnetic elastic intensity at the diagonal incommensurate (DIC) positions $(1, \pm\epsilon, 0)$ decreases as opposed to the increase seen in superconducting samples. This diminution in intensity with increasing magnetic field originates from a spin reorientation transition, which is driven by the antisymmetric exchange term in the spin Hamiltonian. On the other hand, the transition temperature, the incommensurability, and the peak width of the diagonal incommensurate correlations are not changed with magnetic field. This result suggests that the magnetic correlations are determined primarily by the charge disproportionation and that the geometry of the diagonal incommensurate magnetism is also determined by effects, that is, stripe formation which are not purely magnetic in origin. The Dzyaloshinskii-Moriya antisymmetric exchange is nevertheless important in determining the local spin structure in the DIC stripe phase.

PACS numbers: 74.72.Dn, 75.30.Gw, 75.25.+z, 75.50.Lk

I. INTRODUCTION

Extensive elastic neutron scattering studies have been performed on lightly doped $\text{La}_{2-x}\text{Sr}_x\text{CuO}_4$ ($0 \leq x < 0.055$) in order to elucidate the static magnetic properties in the spin-glass regime. The pioneering studies of Wakimoto *et al.* reveal that the static spin correlations in the spin-glass phase show a one-dimensional diagonal spin modulation, in which the direction of the modulation is rotated away by 45° from that in the superconducting phase.^{1,2} In the lightly doped regime $0 \leq x < 0.02$, it is well established that a three-dimensional (3D) antiferromagnetic (AF) long-range ordered phase and a spin-glass phase coexist at low temperatures. Matsuda *et al.* suggested that in this regime electronic phase separation of the doped holes occurs so that some regions with hole concentration $c_h \sim 0.02$ exhibit diagonal stripe correlations while the rest with $c_h \sim 0$ shows 3D AF order.³

One of the remaining puzzles is that the nuclear superlattice peaks, which are predicted by the charge stripe model and are prominent in doped La_2NiO_4 ,⁴ have not been observed in the spin-glass phase of $\text{La}_{2-x}\text{Sr}_x\text{CuO}_4$ although diagonal incommensurate (DIC) magnetic peaks are readily observed. It is, of course, possible that the charge and magnetic stripe model is not cor-

rect. However, there are at least two possibilities to understand the absence of observable nuclear superlattice peaks in $\text{La}_{2-x}\text{Sr}_x\text{CuO}_4$. One is that the peak width is very broad because the charge stripes are significantly disordered. Another is that the peak intensity is extremely low because the coupling between the charge and the lattice is weak. Magnetic field experiments should give valuable information about the origin of the incommensurate magnetic peaks. If the incommensurate peaks are not directly related to underlying charge stripes but rather are purely magnetic in origin, then application of a magnetic field could directly affect the static magnetic order. Magnetic field experiments are also important to understand the role of the magnetic anisotropy as in pure La_2CuO_4 .

It is well known that in pure La_2CuO_4 the net magnetic anisotropy is weakly Ising-like with a strong XY anisotropy and a weaker in-plane Ising anisotropy with the easy-axis along the b axis.⁵ The easy-plane anisotropy in the CuO_2 plane is due to the combination of the spin-orbit and Coulomb exchange interactions.^{6,7} The Dzyaloshinskii-Moriya (D-M) antisymmetric exchange terms are generated by the small rotation of the CuO_6 octahedra, which creates the magnetic anisotropy in the CuO_2 plane as well as the canting of the Cu^{2+} moments

out of the plane.^{8,9} In pure La_2CuO_4 application of a magnetic field perpendicular to the CuO_2 plane causes a first order magnetic transition and, in addition, a weak ferromagnetic component is induced along the magnetic field direction. The magnetic structure also changes from an La_2CuO_4 -type (propagation vector $\boldsymbol{\tau}=\boldsymbol{a}$) to an La_2NiO_4 -type ($\boldsymbol{\tau}=\boldsymbol{b}$) in the high field phase.⁹

With hole doping, the magnetic anisotropy is expected to become smaller since the rotation of the CuO_6 octahedra is reduced. It was previously believed that when the long-range magnetic order disappears at high temperatures or at $x > 0.02$, the magnetic anisotropy plays a less significant role in the magnetic properties. It has been reported, however, that the easy-plane anisotropy is required to describe the L -dependence of the neutron elastic magnetic intensity,^{10,11} in $\text{La}_{2-x}\text{Sr}_x\text{CuO}_4$ for $x \geq 0.02$. It has also been found from magnetization measurements using untwinned crystals that even the easy-axis anisotropy is evident above T_N in crystals with $x=0, 0.01$, and 0.02 and at all temperatures in an $x=0.03$ sample.¹²

In this study we have examined the effect of a magnetic field on the static magnetic correlations in lightly doped $\text{La}_{2-x}\text{Sr}_x\text{CuO}_4$. One important point we wished to clarify is whether the DIC structure is dominated by charge disproportionation or is purely magnetic in origin. It is also important to clarify the nature of the magnetic anisotropy in doped La_2CuO_4 from a microscopic point of view. Although the DIC structure is probably dominated by the charge disproportionation, the static magnetic ordering is in part stabilized by the magnetic anisotropy.

II. EXPERIMENTAL DETAILS

The single crystals of $\text{La}_{2-x}\text{Sr}_x\text{CuO}_4$ ($x=0.014$ and 0.024) were grown by the traveling solvent floating-zone method. The crystals were annealed in an Ar atmosphere at 900°C for 24 h. The uncertainty in the effective hole concentration of each crystal was estimated to be less than 10%. The crystals used in this study were the ones that were employed in the previous neutron-scattering studies.^{3,11} The twin structure of the crystals is shown in Fig. 1. As shown in Fig. 2 of Ref. 2, four twins are possible in the low temperature orthorhombic phase ($Bmab$). A smaller number of twins greatly simplifies the analysis of the incommensurate magnetic peak structure. Fortunately, the $x=0.014$ crystal has a single domain dominant. The $x=0.024$ crystal has two twins, which are estimated to be equally distributed based on the ratio of the nuclear Bragg peak intensities from each twin.

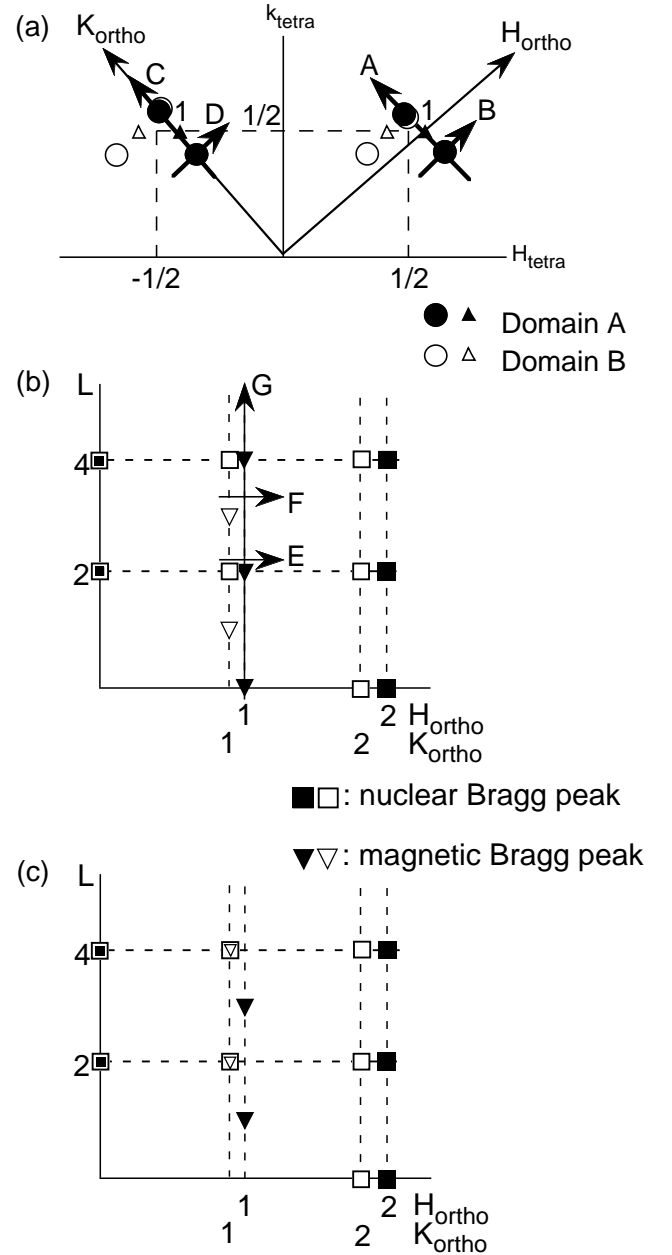


FIG. 1. (a) Diagram of the reciprocal lattice in the $(HK0)$ scattering zone. Filled and open symbols are for domains A and B, respectively. The circles and triangles correspond to the incommensurate magnetic peaks and fundamental Bragg peaks, respectively. (b) Diagram of the reciprocal lattice in the $(H0L)$ scattering zone. The magnetic reflections predicted from the La_2CuO_4 -type structure are shown. Filled and open symbols are for domains A and B, respectively. The triangles and squares correspond to the magnetic peaks and nuclear Bragg peaks, respectively. (c) The magnetic reflections predicted from the La_2NiO_4 -type structure are shown.

The neutron-scattering experiments were carried out on the cold neutron three-axis spectrometer LTAS and the thermal neutron three-axis spectrometer TAS2 installed in the guide hall of JRR-3M at the Japan Atomic Energy Research Institute. Typical horizontal collimator

sequences were guide-80'-S-20'-80' with a fixed incident neutron energy of $E_i=5.05$ meV at LTAS and guide-40'-S-40'-80' with a fixed incident neutron energy of $E_i=13.7$ meV at TAS2. Contamination from higher-order beams was effectively eliminated using Be filters at LTAS and pyrolytic graphite filters at TAS2. The single crystals were oriented in the $(HK0)_{\text{ortho}}$ or $(H0L)_{\text{ortho}}$ scattering plane. The neutron-scattering experiments in a magnetic field were performed up to 10 T using a new type of split-pair superconducting magnet cooled by cryocoolers. The field was applied perpendicular to the scattering plane. In this paper, we use the low temperature orthorhombic phase ($Bmab$) notation $(h, k, l)_{\text{ortho}}$ to express Miller indices.

III. RESULTS

A. Magnetic field perpendicular to the CuO_2 plane

1. $\text{La}_{1.986}\text{Sr}_{0.014}\text{CuO}_4$ (Néel ordered phase)

The effect of a magnetic field was studied first in $\text{La}_{1.986}\text{Sr}_{0.014}\text{CuO}_4$, which exhibits coexistence of a 3D Néel ordered phase and a quasi-2D spin-glass phase at low temperatures.³ Figure 2 shows the magnetic field dependence of the magnetic Bragg intensity at $(1,0,0)$ in $\text{La}_{1.986}\text{Sr}_{0.014}\text{CuO}_4$. The magnetic field is applied perpendicular to the CuO_2 plane. At 50 K the $(1,0,0)$ magnetic Bragg intensity, originating from the long-range AF ordering, gradually decreases with increasing magnetic field and shows a sharp drop at a critical field of 4.4 T. The magnetic structure factor of the $(1,0,0)$ reflection becomes zero because a spin reorientation transition from the La_2CuO_4 -type magnetic structure to the La_2NiO_4 -type magnetic structure occurs.⁹ In this transition the spins in the orthorhombic unit cell at $(0,0,0)$ ($S\|\mathbf{b}$) and $(\frac{1}{2}, \frac{1}{2}, 0)$ ($\|\mathbf{-b}$) are unchanged at H_c but those at $(0, \frac{1}{2}, \frac{1}{2})$ ($\|\mathbf{b}$) and $(\frac{1}{2}, 0, \frac{1}{2})$ ($\|\mathbf{-b}$) for $H < H_c$ change sign above H_c . This critical field is comparable to that in $\text{La}_2\text{CuO}_{4+\delta}$, which also has a similar Néel temperature $T_N=234$ K.⁹

With decreasing temperature, the critical field becomes larger. At the same time, magnetic hysteresis occurs between the field increasing and field decreasing processes as shown in Fig. 2(a). We confirmed that this behavior is reproducible. A characteristic feature is that the intensity at $(1,0,0)$ does not return to the initial value even at 0 T after the magnetization cycle. Such large hysteresis behavior at $(1,0,0)$ was not observed in $\text{La}_2\text{CuO}_{4+\delta}$.⁹ A possible origin will be discussed in Sec. 4.

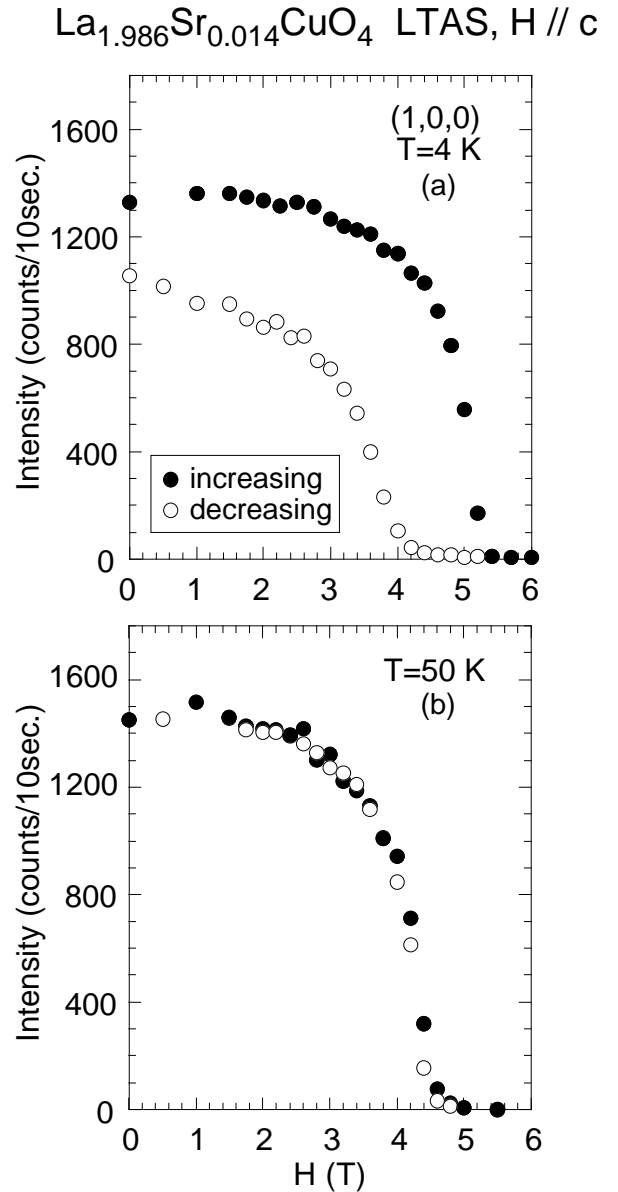


FIG. 2. Magnetic field dependence of the $(1,0,0)$ magnetic Bragg intensity at 4 K and 50 K in $\text{La}_{1.986}\text{Sr}_{0.014}\text{CuO}_4$. Magnetic field is applied perpendicular to the CuO_2 plane.

La_{1.986}Sr_{0.014}CuO₄ LTAS, H // c, T=4 K

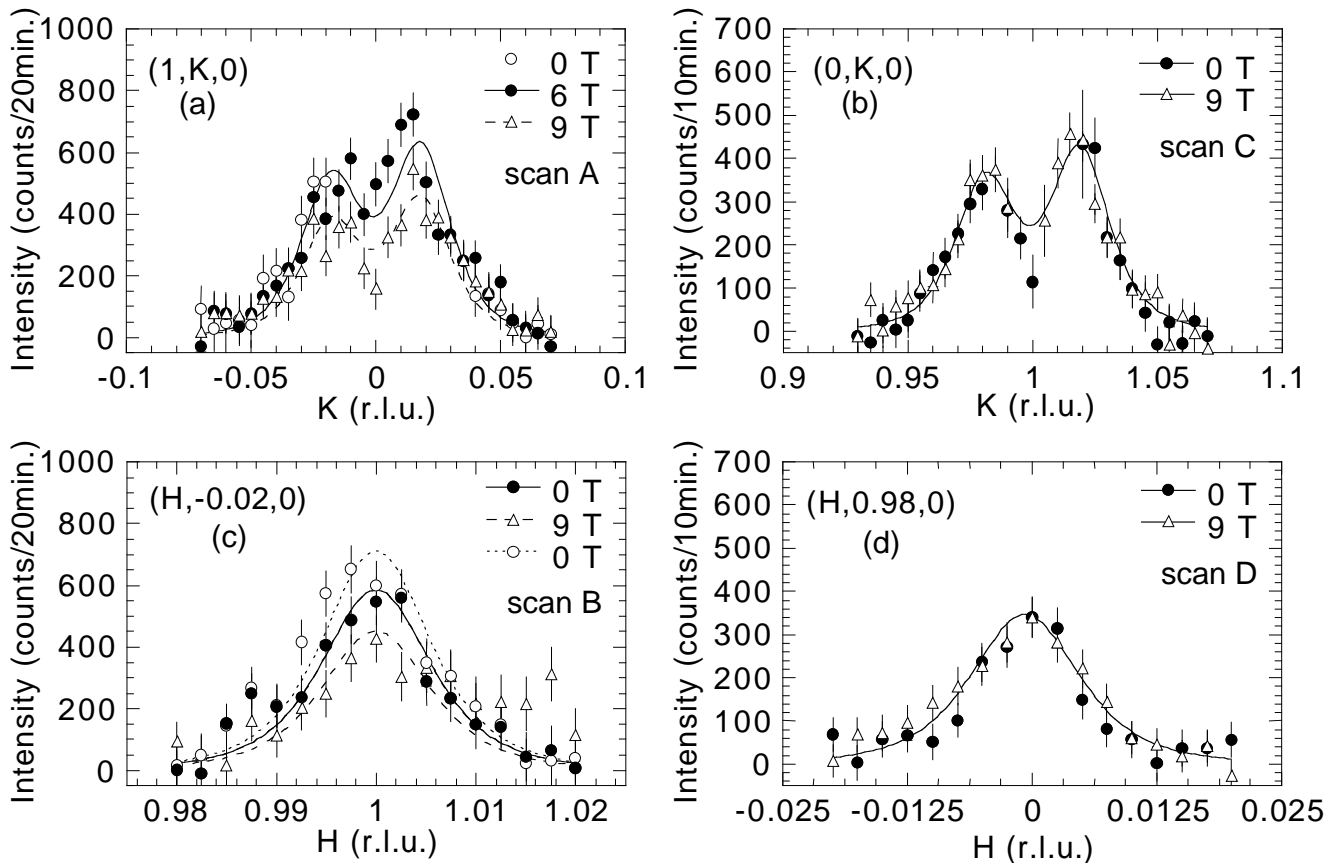


FIG. 3. Magnetic elastic intensity around the diagonal incommensurate positions $(1, \pm\epsilon, 0)$ and $(0, 1 \pm \epsilon, 0)$ at 4 K in $\text{La}_{1.986}\text{Sr}_{0.014}\text{CuO}_4$ as a function of magnetic field. The scan trajectories are shown in Fig. 1(a). Open circles in (c) are the data measured at 0 T after a magnetization cycle. Magnetic field is applied perpendicular to the CuO_2 plane. Background intensities measured at a high temperature have been subtracted. The lines are guides to the eyes.

2. $\text{La}_{1.986}\text{Sr}_{0.014}\text{CuO}_4$ (spin-glass phase)

Figure 3 shows the magnetic field dependence of the magnetic elastic intensity around the DIC positions $(1, \pm\epsilon, 0)$ and $(0, 1 \pm \epsilon, 0)$ in $\text{La}_{1.986}\text{Sr}_{0.014}\text{CuO}_4$. The magnetic signal, which develops below ~ 30 K, originates from the phase-separated spin-glass regions. The incommensurate peaks are asymmetric because of the twin structure as shown in Fig. 1(a). The peak profiles are consistent with those observed in the previous measurements at zero field.³ Below H_c there exists an intense magnetic Bragg peak at $(1, 0, 0)$ so that the data around $(1, 0, 0)$ are contaminated. On the other hand, above H_c , the data around $(0, 1, 0)$ are contaminated because of double scattering at the $(0, 1, 0)$ magnetic peak position. This double scattering is made allowed by the transition to the La_2NiO_4 -type magnetic structure at high field. As shown in Fig. 3(a), the magnetic intensities at $(1, \pm\epsilon, 0)$ are almost constant between 0 and 6 T and gradually

decrease above 6 T. Since the $(1, 0, 0)$ peak in the Néel ordered phase shows a decrease with increasing field, it is natural to think that the decrease of the DIC peak intensity also originates from the spin reorientation transition. As shown in Fig. 2, $H_c = 5.2$ T at 4 K in the Néel ordered phase, indicating that the averaged transition field is similar, albeit somewhat larger, in the spin-glass phase. The transition is very broad in the spin-glass phase because the cluster size is finite and, in particular, there is only short range magnetic order (~ 10 Å) between the CuO_2 planes. This result is consistent with that of magnetization measurements, which shows a broadening of the jump in the magnetization at H_c .¹³

The magnetic intensity at $(0, 1 \pm \epsilon, 0)$ is almost magnetic field independent as shown in Figs. 3(b) and 3(d). The magnetic signal at $(0, 1 \pm \epsilon, 0)$ may be considered to be the tail of $(0, 1 \pm \epsilon, 1)$, which is broadened along the c axis because of the quasi-2D nature of the DIC state.¹¹ The instrumental resolution which is elongated vertically in-

tegrates the tail effectively. The (0,1,1) magnetic Bragg peak should decrease in intensity under magnetic field, whereas the (0,1,0) magnetic intensity increases. Both contributions will tend to compensate each other, so that the intensity at $(0,1\pm\epsilon,0)$ may remain almost unchanged.

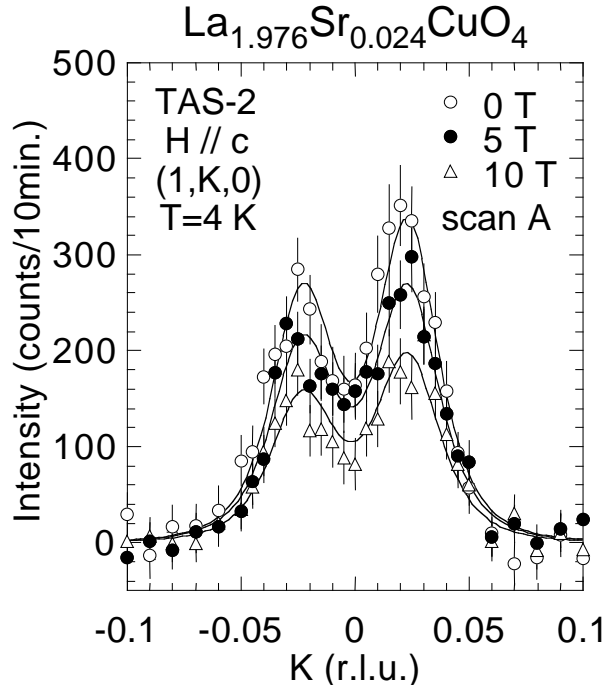


FIG. 4. Magnetic elastic intensity around the diagonal incommensurate positions $(1,\pm\epsilon,0)$ at 4 K in $\text{La}_{1.976}\text{Sr}_{0.024}\text{CuO}_4$ as a function of magnetic field. The scan trajectory is shown in Fig. 1(a). Magnetic field is applied perpendicular to the CuO_2 plane. Background intensities measured at a high temperature have been subtracted. The solid lines are guides to the eyes.

3. $\text{La}_{1.976}\text{Sr}_{0.024}\text{CuO}_4$ (spin-glass phase)

The effect of a magnetic field has also been studied in $\text{La}_{1.976}\text{Sr}_{0.024}\text{CuO}_4$. At zero field, this sample shows no long-range AF order but only diagonal stripe spin-glass behavior below ~ 25 K. Figure 4 shows the effect of a magnetic field in $\text{La}_{1.976}\text{Sr}_{0.024}\text{CuO}_4$ with the field perpendicular to the CuO_2 plane. The magnetic intensity at $(1,\pm\epsilon,0)$ decreases monotonically with increasing magnetic field. The tendency is similar to that in $\text{La}_{1.986}\text{Sr}_{0.014}\text{CuO}_4$ although the overall effect is much more gradual presumably because the between-plane magnetic correlation length is only 3 Å. Since this sample shows only spin-glass ordering at low temperatures, the $(1,0,0)$ magnetic Bragg peak is absent and the DIC peaks per unit sample volume are more intense than those in the $x=0.014$ sample. Therefore, the magnetic field dependence of the DIC peaks can be clearly observed in this sample. We found, in addition, that the

transition temperature, the peak width, and peak positions are almost unchanged under magnetic field.

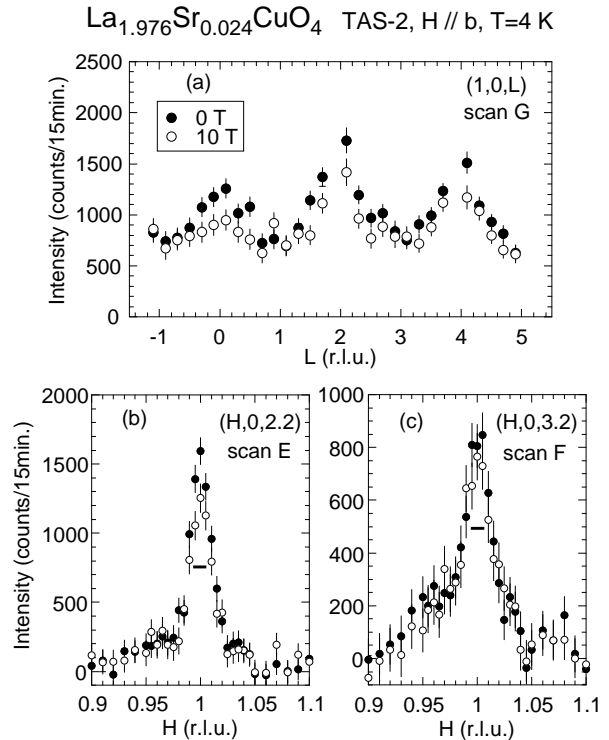


FIG. 5. Magnetic elastic intensity at $(1,0,L)$, $(H,0,2.2)$, and $(H,0,3.2)$ at 4 K in $\text{La}_{1.976}\text{Sr}_{0.024}\text{CuO}_4$ as a function of magnetic field. The scan trajectories are shown in Fig. 1(b). Magnetic field is parallel to the CuO_2 plane. Background intensities measured at a high temperature have been subtracted. The horizontal bars in (b) and (c) represent the instrumental resolution.

B. Magnetic field parallel to the CuO_2 plane

We have so far discussed only the effects of a magnetic field when the field is applied perpendicular to the CuO_2 plane. Figure 5 shows the effect of the magnetic field applied parallel to the CuO_2 plane in $\text{La}_{1.976}\text{Sr}_{0.024}\text{CuO}_4$. The scan along $(1,0,L)$ shows broad peaks at the $L = \text{even}$ positions in zero field;¹⁰ these are the positions where magnetic Bragg peaks are observed in pure La_2CuO_4 . The peaks are broad because the correlation length along the c axis is very short as noted above. The magnetic peaks in Figs. 5(b) and 5(c) are asymmetric and have a tail at lower Q 's because of the twin structure as shown in Fig. 1(b). The peak profiles are consistent with those observed in the previous measurements at zero field.¹⁰

Under a magnetic field of 10 T, the peak widths along the a , b , and c axes are unchanged, indicating that magnetic correlation length is not measurably affected. On the other hand, the magnetic intensity decreases over a

wide range of L . In $\text{La}_2\text{CuO}_{4+\delta}$, a spin-flop transition, which is due to the D-M exchange, occurs when the magnetic field is applied along the easy-axis b .¹⁴ Above the transition field, which is about twice as large as that observed for $\mathbf{H}\parallel\mathbf{c}$, spin components along the a and c axes appear. This explains the decrease in magnetic intensity at $(1,0,L)$ qualitatively.

Thus, the magnetic elastic signal decreases under magnetic field irrespective of the field direction. This result with $x=0.024$ sample is consistent with that expected from a broadened spin reorientation transition, originating from the D-M exchange interaction, in analogy to the first order transition in $\text{La}_2\text{CuO}_{4+\delta}$. Again, the transition is severely broadened because of the very short between-plane correlation length.

IV. DISCUSSION AND CONCLUSIONS

Our elastic neutron-scattering study in lightly doped $\text{La}_{2-x}\text{Sr}_x\text{CuO}_4$ reveals that the magnetic field affects the direction which the spins point along. On the other hand, the transition temperature, the peak width, and the incommensurability are almost unaffected. This result suggests that the magnetic correlations are dominated by the charge disproportionation rather than magnetic interaction effects.

We have found that the DIC structure in the spin-glass phase has an in-plane Ising anisotropy originating from a combination of XY anisotropy and the D-M antisymmetric exchange as in pure La_2CuO_4 . This result is consistent with that in the magnetization measurements,¹² which suggests that the in-plane magnetic anisotropy continues to play an important role even after the Néel order is destroyed. It should be emphasized that our study evinced the in-plane magnetic anisotropy specifically in the DIC phase. This magnetic anisotropy plays an important role in determining the spin direction in the DIC structure. Since the rotation of the CuO_6 octahedra is larger in the lower hole concentration region, the D-M antisymmetric exchange will be more pronounced in the lower hole concentration region. It has been reported previously that the static DIC spin modulation is stabilized in the lower hole concentration region.³ This is partly because the diagonal stripe is increasingly stabilized as the rotation of the CuO_6 octahedra becomes larger in the $Bmab$ phase. However, since the magnetic anisotropy, which reduces quantum spin fluctuations, enhances hole attraction and stabilizes magnetic order,^{15,16,17} the static DIC structure in $\text{La}_{2-x}\text{Sr}_x\text{CuO}_4$ may also be influenced by the magnetic anisotropy. It would be interesting to observe directly the energy gap in the spin excitations due to the magnetic anisotropy at the magnetic zone center. However, the peak width in energy becomes so broad that the anisotropy gap energy is very difficult to determine experimentally.¹¹

The magnetic anisotropy in lightly doped

$\text{La}_{2-x}\text{Sr}_x\text{CuO}_4$ should be taken into account in determining the appropriate spin structure model in the spin-glass phase. The L -dependence of the magnetic intensity, shown in Fig. 5(a), can be described by 3D correlated AF spin clusters with the spin randomly oriented within the ab plane and with $\boldsymbol{\tau}(\parallel\mathbf{a})$. Alternatively, the data are consistent with equal admixtures of 3D correlated phases where the spin vector \mathbf{S} is along or perpendicular to $\boldsymbol{\tau}(\parallel\mathbf{a})$.¹⁰ It should be noted that all the spins point along the b axis in excess-oxygen-doped $\text{La}_2\text{CuO}_{4+y}$, which shows a parallel incommensurate magnetic modulation below ~ 42 K.¹⁸

Lee *et al.* suggested that the weak ferromagnetic moment in each CuO_2 plane, originating from the out-of-plane spin canting, is absent in $\text{La}_2\text{CuO}_{4+y}$ because in the stripe model, in which there exist antiphase domain boundaries between ordered spins, the out-of-plane spin canting points in opposite directions on either side of a domain wall.¹⁸ Then, the size of the magnetic field effect would be inversely related to the number of antiphase domains inside of a magnetically correlated area, suggesting that the decrease in magnetic intensity in a magnetic field should become smaller as the Sr-doping gets larger. There may, of course, be additional magnetic mechanisms, in addition to the one we have identified, contributing to the diminution of the DIC magnetic peak intensity under the application of a magnetic field.

The effects of a magnetic field have also been studied in superconducting $\text{La}_{2-x}\text{Sr}_x\text{CuO}_4$ ($x=0.10$ and 0.12) and excess-oxygen-doped $\text{La}_2\text{CuO}_{4+y}$. It has been found that the static parallel stripe magnetic order is enhanced under the application of a magnetic field perpendicular to the CuO_2 planes.^{19,20,21} This is completely opposite to our result in lightly doped $\text{La}_{2-x}\text{Sr}_x\text{CuO}_4$. The enhancement of the elastic magnetic intensity is ascribed to the vortices which stabilize the static magnetic order over a region much larger than the vortex cores.^{19,20,21} Our results indirectly support this interpretation.

We now discuss the magnetic hysteresis behavior in $\text{La}_{1.986}\text{Sr}_{0.014}\text{CuO}_4$. The hysteresis behavior becomes pronounced with decreasing temperature below 50 K. This can be related to the spin-glass behavior. As shown in Fig. 3(c), the magnetic intensity at $(1,-0.02,0)$ increases slightly after a magnetization cycle. The slight increase in magnetic intensity after the magnetization cycle is probably related to the $(1,0,0)$ magnetic Bragg intensity lost after the cycle, as shown in Fig. 2(a). However, the increased intensity at $(1,-0.02,0)$ is factor of ~ 30 smaller than the lost intensity at $(1,0,0)$. Therefore, some fraction of the Néel ordered phase still remains in the La_2NiO_4 -type structure after the magnetization cycle.

In summary, our neutron-scattering experiments under magnetic field demonstrate the effects of the D-M interaction in the spin-glass phase in lightly doped $\text{La}_{2-x}\text{Sr}_x\text{CuO}_4$. Although the DIC structure regimes are determined by the charge disproportionation, the static magnetic ordering is stabilized in part by the magnetic

anisotropy.

ACKNOWLEDGMENTS

We would like to thank S. Katano, Y. S. Lee, T. Suzuki, and S. Wakimoto for stimulating discussions and Y. Shimojo for technical assistance. This study was supported in part by the U.S.-Japan Cooperative Program on Neutron Scattering, by a Grant-in-Aid for Scientific Research from the Japanese Ministry of Education, Science, Sports and Culture, by a grant for the promotion of science from the Science and Technology Agency, and by CREST. Work at Brookhaven National Laboratory was carried out under Contract No. DE-AC02-98CH10886, Division of Material Science, U.S. Department of Energy. Work at the University of Toronto is part of the Canadian Institute for Advanced Research and is supported by the Natural Science and Engineering Research Council of Canada.

- ¹² A. N. Lavrov, Y. Ando, S. Komiya, and I. Tsukada, *Phys. Rev. Lett.* **87**, 017007 (2001).
- ¹³ T. Suzuki, unpublished.
- ¹⁴ T. Thio, C. Y. Chen, B. S. Freer, D. R. Gabbe, H. P. Jenssen, M. A. Kastner, P. J. Picone, N. W. Preyer, and R. J. Birgeneau, *Phys. Rev. B* **41**, 231 (1990).
- ¹⁵ J. Riera and E. Dagotto, *Phys. Rev. B* **47**, 15346 (1993).
- ¹⁶ A. L. Chernyshev and P. W. Leung, *Phys. Rev. B* **60**, 1592 (1999).
- ¹⁷ J. A. Riera, *Phys. Rev. B* **64**, 104520 (2001).
- ¹⁸ Y. S. Lee, R. J. Birgeneau, M. A. Kastner, Y. Endoh, S. Wakimoto, K. Yamada, R. W. Erwin, S.-H. Lee, and G. Shirane, *Phys. Rev. B* **60**, 3643 (1999).
- ¹⁹ S. Katano, M. Sato, K. Yamada, T. Suzuki, and T. Fukase, *Phys. Rev. B* **62**, R14677 (2000).
- ²⁰ B. Lake, H. M. Rønnow, N. B. Christensen, G. Aeppli, K. Lefmann, D. F. McMorrow, P. Vorderwisch, P. Smeibidl, N. Mangkorntong, T. Sasagawa, M. Nohara, H. Takagi, and T. E. Mason, *Nature* **415**, 299 (2002).
- ²¹ B. Khaykovich, Y. S. Lee, R. Erwin, S.-H. Lee, S. Wakimoto, K. J. Thomas, M. A. Kastner, and R. J. Birgeneau, *Phys. Rev. B* **66**, 014528 (2002).

-
- ¹ S. Wakimoto, G. Shirane, Y. Endoh, K. Hirota, S. Ueki, K. Yamada, R. J. Birgeneau, M. A. Kastner, Y. S. Lee, P. M. Gehring, and S. H. Lee, *Phys. Rev. B* **60**, R769 (1999).
 - ² S. Wakimoto, R. J. Birgeneau, M. A. Kastner, Y. S. Lee, R. Erwin, P. M. Gehring, S. H. Lee, M. Fujita, K. Yamada, Y. Endoh, K. Hirota, and G. Shirane, *Phys. Rev. B* **61**, 3699 (2000).
 - ³ M. Matsuda, M. Fujita, K. Yamada, R. J. Birgeneau, Y. Endoh, and G. Shirane, *Phys. Rev. B* **65**, 134515 (2002).
 - ⁴ J. M. Tranquada, D. J. Buttrey, V. Sachan, *Phys. Rev. B* **54**, 12318 (1996).
 - ⁵ C. J. Peters, R. J. Birgeneau, M. A. Kastner, H. Yoshizawa, Y. Endoh, J. Tranquada, G. Shirane, Y. Hidaka, M. Oda, M. Suzuki, and T. Murakami, *Phys. Rev. B* **37**, 9761 (1988).
 - ⁶ T. Yildirim, A. B. Harris, A. Aharony, and O. Entin-Wohlman, *Phys. Rev. B* **52**, 10239 (1995).
 - ⁷ O. Entin-Wohlman, A. B. Harris, and A. Aharony, *Phys. Rev. B* **53**, 11661 (1996).
 - ⁸ T. Thio, T. R. Thurston, N. W. Preyer, P. J. Picone, M. A. Kastner, H. P. Jenssen, D. R. Gabbe, C. Y. Chen, R. J. Birgeneau, and A. Aharony, *Phys. Rev. B* **38**, 905 (1988).
 - ⁹ M. A. Kastner, R. J. Birgeneau, T. R. Thurston, P. J. Picone, H. P. Jenssen, D. R. Gabbe, M. Sato, K. Fukuda, S. Shamoto, Y. Endoh, K. Yamada, and G. Shirane, *Phys. Rev. B* **38**, 6636 (1988).
 - ¹⁰ M. Matsuda, Y. S. Lee, M. Greven, M. A. Kastner, R. J. Birgeneau, K. Yamada, Y. Endoh, P. Böni, S.-H. Lee, S. Wakimoto, and G. Shirane, *Phys. Rev. B* **61**, 4326 (2000).
 - ¹¹ M. Matsuda, M. Fujita, K. Yamada, R. J. Birgeneau, M. A. Kastner, H. Hiraka, Y. Endoh, S. Wakimoto, and G. Shirane, *Phys. Rev. B* **62**, 9148 (2000).